Computer Methods and Programs in Biomedicine 191 (2020) 105412

Contents lists available at ScienceDirect

Computer Methods and Programs in Biomedicine

journal homepage: www.elsevier.com/locate/cmpb

Gompertz tracking of the growth trajectories of the human-liver-cancer xenograft-tumors in nude mice

Dongdong Yang[a], Ping Gao[a,*], Chao Tian[b,c,*], Yang Sheng[b,c,*]

[a] School of Life Sciences, University of Science and Technology of China, Hefei 230027, China
[b] School of Engineering Science, University of Science and Technology of China, Hefei 230027, China
[c] Key Laboratory of Precision Scientific Instrumentation of Anhui Higher Education Institutes, University of Science and Technology of China, Hefei 230027, China

ARTICLE INFO

Article history:
Received 29 November 2019
Revised 8 February 2020
Accepted 19 February 2020

Keywords:
Gompertz
Gsk3β
c-Myc
Liver cancer
Xenograft tumor

ABSTRACT

Background and objective: The accurate tracking of the growth trajectories of the human-liver-cancer xenograft-tumors in nude mice is an important prerequisite for the effective use of relevant trial results. Our objective is first to find out whether the Gompertz model can accurately track the growth trajectories of the xenograft-tumors in the non-target control group, Gsk3β knockdown, and c-Myc knockdown groups; secondly, to verify the effect of knocking down Gsk3β or c-Myc on the growth of xenograft-tumors and reveal the mechanism; finally, to demonstrate the 100-day Gompertz growth trajectory, which is a complete growth process with two phases and three stages.

Methods: The 18 male specific-pathogen-free (SPF) BALB/c nude mice were randomly divided into three groups and different interventions were performed to establish the non-target control, Gsk3β knockdown, and c-Myc knockdown groups. The volumes of the xenograft-tumors were measured from day 14 to day 30 after transplantation. The first 30-days and the whole 100-days of Gompertz growth trajectories of the xenograft-tumors were obtained respectively, and the growth assessment indicators of each group were calculated based on the parameters of the Gompertz model.

Results: 1) The Gompertz model can accurately track the growth trajectories of xenograft-tumors in the non-target control, Gsk3β knockdown, and c-Myc knockdown groups; 2) knocking down Gsk3β or c-Myc can inhibit the growth of xenograft-tumors. It is the combined effect of growth-promoting factor, growth inhibitory factor, and the delay of angiogenesis, of which the delay of angiogenesis plays a decisive role; 3) the 100-day Gompertz growth trajectory can provide complete information about the two phases and three stages of xenograft-tumor growth. Therefore, it is strongly recommended that nude mouse trials be extended from 30 days (currently widely accepted) to 100 days.

Conclusions: The Gompertz model can well reveal the growth pattern of the human-liver-cancer xenograft-tumors in nude mice. Combined with the growth assessment indicators obtained from the Gompertz model parameters, one can further clarify the mechanism that affects the growth of xenograft-tumors. The Gompertz tracking of the growth trajectories of the human-liver-cancer xenograft-tumors in nude mice has broad application prospects in the fields of basic research, drug verification, and clinical treatment, etc.

1. Introduction

The Gompertz model was created by Benjamin Gompertz (1825) to describe human mortality and establish an actuarial table [1]. Laird AK (1964) pioneered the study of fitting tumor growth data using the Gompertz model [2]. It is well known that the growth of solid tumors progresses through two distinct phases: the avascular phase and the vascular phase [3,4]. To date, the accuracy of the Gompertz model in modeling avascular tumor growth has been widely recognized [5,6]. Tumor angiogenesis is initiated by its release of certain chemicals called tumor angiogenic factors (TAF) [7]. Once blood vessels have formed, the volume and mass of the tumor increase rapidly. The growth pattern of vascularized tumors becomes complicated due to the interaction between blood vessels, tumors, and the surrounding tissues [7,8]. In vitro,

* Corresponding authors.
E-mail addresses: yangdd@ustc.edu.cn (D. Yang), pgao2@ustc.edu.cn (P. Gao), ctian@ustc.edu.cn (C. Tian), yangs@ustc.edu.cn (Y. Sheng).

https://doi.org/10.1016/j.cmpb.2020.105412
0169-2607/

preclinical and clinical studies have shown that the Gompertz model of fixed parameters can still accurately fit the growth data of vascularized tumors in the same type of host if it is not disturbed during growth [9]. The treatment of vascularized tumors is a highly complex, multi-step process that depends on many determinants, so it is a very difficult task to establish a Gompertz model of tumor growth under therapeutic intervention. Some important advances in the Gompertz modeling of vascularized tumor growth under therapeutic intervention have also been reported. Philip Hahnfeldt et al. accurately described the treatment response under the control of angiogenic stimulator and inhibitor by modifying the Gompertz model with a variable carrying capacity instead of a fixed carrying capacity [8]. Niklas Hartung et al. verified that the Gompertz model can predict tumor growth and metastatic spreading in tumor-bearing mice [10]. Sebastien Benzekry et al. assessed the ability of the Gompertz model to predict future tumor growth [11]. Spyridon Patmanidis et al. focused on estimating the parameters of the Gompertz model and believe that in most cases the Maximum Likelihood estimator is able to provide more reliable predictions for the tumor's growth on individual test subjects [12]. The current development trend of the Gompertz model for vascularized tumor treatment is to replace its fixed parameters with time-varying parameters or to introduce a delay on the time axis [13–15].

Gene therapy is a precise therapeutic intervention at the molecular level, which has promoted the development of the concepts of "individualization" and "precise medicine", and is a very promising method for tumor biotherapy [16–18]. The need for technology advancement in tumor gene therapy brings new challenges to the tumor's Gompertz modeling. Glycogen synthetic kinase 3β (Gsk3β) has complex biological functions and plays a regulatory role in transcribing tumor cell genes, accelerating cell cycle, participating in tumor cell invasion, metastasis and apoptosis [19,20]. Gsk3β plays different roles in different tumors and may become a potential target for tumor treatment. The abnormal expression of Gsk3β promotes cell growth in some tumors but inhibits cell growth in other tumors. Cellular-myelocytomatosis (c-Myc) is one of the most common activated oncogenes in the occurrence and development of human liver cancer and is involved in a variety of biological processes such as cell growth, apoptosis, and metabolism. The expression of the c-Myc protein is significantly increased in most liver cancer patients. Down-regulating the expression of a c-Myc gene can inhibit the proliferation of liver cancer cells. A pharmacologically feasible c-Myc targeting method will represent a new treatment model for liver cancer [21]. In the study of knocking down Gsk3β or knocking down c-Myc to inhibit the growth of human-liver-cancer xenograft-tumors in nude mice, we found that both interventions can inhibit the growth of xenograft-tumors at an early stage and accelerate their growth at a later stage, which is very confusing and has not been explained well in theory. The effect of knocking down Gsk3β or c-Myc on the growth of liver cancer is a scientific issue worthy of further investigation, which directly relates to whether these two tumor gene therapy methods can enter the clinical application as soon as possible.

In this study, we will use the Gompertz model to track the growth trajectories of the vascularized human-liver-cancer xenograft-tumors in nude mice, including the non-target control, Gsk3β knockdown and c-Myc knockdown groups. Based on the parameters of the Gompertz model estimated by the Levenberg-Marquardt nonlinear regression algorithm, the quantitative assessment indicators reflecting the growth promotion or inhibition of xenograft-tumors will be calculated. Our study has the following objectives: first, to find out whether Gompertz model can accurately track the growth trajectories of the xenograft tumors in the non-target control group, Gsk3β knockdown, and c-Myc knockdown groups; secondly, to verify the effect of knocking down Gsk3β or c-Myc on the growth of xenograft-tumors and reveal the mechanism; finally, to demonstrate the 100-day Gompertz growth trajectory, which is a complete growth process with two phases and three stages.

The rest of this paper is organized as follows: In Section 2, we make an ethical statement and then detail the establishment of the nude mouse models of the non-target control group, Gsk3β knockdown, and c-Myc knockdown groups. Subsequently, we introduce the differential equations, analytical solutions, and the Levenberg-Marquardt parameter estimation method for the Gompertz model. In Section 3, we present the growth trajectories and residuals tracked by the Gompertz model, calculate the growth-promoting factors, growth inhibitory factors, and carrying capacities, and then extend the growth trajectories of xenograft-tumors from 30 days to 100 days. In Section 4, we discuss the inability of a vernier caliper to measure the volume of avascular xenograft-tumors, the two key prerequisites for obtaining high-quality growth trajectories, the effect of delaying the angiogenesis of xenograft tumors, the mechanism of knocking down Gsk3β or c-Myc to inhibit the growth of xenograft tumors, and the advantages of the 100-day Gompertz growth trajectories. In Section 5, we will summarize the work of this paper, clarify how the results support our objectives and point out the academic value and application prospects of this study.

2. Material and methods

2.1. Ethics statement

All trials on the human-liver-cancer xenograft-tumors in nude mice were approved by the Animal Use and Management Committee of the University of Science and Technology of China, in line with international practices and the relevant national regulations of the People's Republic of China.

2.2. Nude mouse model of human-liver-cancer xenograft-tumor

Nude mice are congenital hairless, thymus-free, completely deficient in T lymphocyte function, and do not cause xenograft-tumor rejection [22–24]. Therefore, xenograft-tumors can grow well and are easily observed with the naked eyes. Nude mouse models of human-liver-cancer xenograft-tumor are established by the direct transplantation of human-liver-cancer cell lines or tissue blocks into nude mice. The establishments of the human-liver-cancer xenograft-tumor models in nude mice make it possible to study the human-liver-cancer in animals and maintain the morphology, function, and secretion of alpha-fetoprotein (AFP) in primary human-liver-cancer. It is one of the models closest to primary human-liver-cancer and is commonly used to screen anti-tumor drugs and preparations, to experimentally treat tumors and study anti-tumor mechanisms. The quality of the tumor-derived cells, subcutaneous transplantation time, subcutaneous injection methods and surgical techniques all have a significant impact on the success rate of primary transplantation [25–29].

Eighteen male specific-pathogen-free (SPF) BALB / c nude mice, born 4–5 weeks, weighing 18–20 g, were purchased from the Nanjing Biomedical Research Institute of Nanjing University (NBRI). Under the condition of SPF, they were individually raised in cages at the Experimental Animal Center of the University of Science and Technology of China. The eighteen nude mice were randomly divided into three groups to establish different trial models: non-target control, Gsk3β knockdown, and c-Myc knockdown groups.

The transplantation date was specified as day 0. The state of the mouse was observed every 2–3 days, and the tumor was measured for the first time on day 14. After that, the body weights and tumor volumes of each group were recorded simultaneously every three days. The long radius b and short radius a of the tumor were

measured with a vernier caliper, and the tumor volumes were calculated by using the formula $V = 4\pi a^2 b/3$.

2.3. Gompertz model and its parameter estimation

The differential equation of the Gompertz model for the growth of a xenograft-tumor is

$$\begin{cases} dV(t)/dt = rV(t) \cdot (\ln K - \ln V(t)) \\ V(t_0) = V_0 \end{cases}$$

where $V(t)$ is the volume of the xenograft-tumor at time t and cannot be equal to zero (the logarithm of zero does not exist), i.e., the xenograft-tumor must have a certain size; V_0 is the initial volume of the xenograft-tumor, and it should be chosen carefully because its measurement error is critical for the accurate estimation of the parameters; Many researchers refer to r as the intrinsic growth rate. In fact, it inhibits growth during the exponential and linear growth stage of the xenograft-tumor (on the premise of keeping other parameters unchanged, the greater the value, the stronger the ability to inhibit the xenograft-tumor growth); K is the carrying capacity of a nude mouse, i.e., the maximum volume of the xenograft-tumor in the plateau stage; $r\ln K$ is an important indicator for assessing the ability to promote the xenograft-tumor growth (on the premise of keeping other parameters unchanged, the greater the value, the stronger the ability to promote the xenograft-tumor growth). The analytical solution of the differential equation is

$$V(t) = Kexp((\ln(V_0/K)) \cdot exp(-r(t - t_0)))$$

In the above formula, the parameters r and K need to be estimated from the measured data of the xenograft-tumor volume. The traditional parameter estimation method is to linearize the formula first, then use the least-squares method to estimate, and finally convert the formula back [30–32]. To fit the Gompertz model using the least-squares method, the model needs to be linearized first; at the same time, this process will make the systematical and random errors in the measurement data become nonlinear, which is harmful to the least-squares solution. In addition, the model is linearized first and then converted back to the non-linear Gompertz model after the least-squares fit. These two steps also introduce calculation errors. Nonlinear regression is the development trend of the parameter estimation in the Gompertz model. We use the Levenberg-Marquardt (LM) algorithm to estimate the parameters r and K [33–35]. At present, we can reduce the maximum residual of the Levenberg-Marquardt algorithm to less than 24.68% of that of the least-square method. Due to the strong correlation between the parameters r and K, only a small number of measured data points of the xenograft-tumor volume are required to obtain sufficiently accurate estimates of the parameters r and K.

The Levenberg-Marquardt (LM) algorithm is an improved form based on the Gauss-Newton method. It has both the local features of the Gauss-Newton method and the global features of the gradient method. It uses the approximate second-order derivative information, which is faster than the gradient method. Moreover, its algorithm is more robust.

The Levenberg-Marquardt algorithm starts with the initial guess $x_0=[V_0{}^0, K^0, r^0]$. $x=[V_0, K, r]$ is adjusted by the search step size δ only for downhill steps.

$$\left(J^T J + \lambda I\right)\delta = J^T R_e$$

J = Jacobian matrix of the residual derivatives to the parameters
λ = damping parameter (adaptive balance); R_e= a residual vector.

2.3.1. Calculation process of the Levenberg–Marquardt algorithm

2.3.1.1. Initialization. Initialize values for the parameters, x, the Levenberg–Marquardt parameter λ, as well as λ_{up} and λ_{down} for adjusting the damping term. Evaluate the residuals R_e and the Jacobian J at the initial parameter guess.

2.3.1.2. Matrix and gradient. Calculate the matrix, $g=J^T J+\lambda I$, and the cost gradient, $\nabla C = J^T R_e$, $C = \frac{1}{2}R_e{}^2$.

2.3.1.3. Residual and cost. Estimate the new residuals R_{enew} at the point given by $x_{new} = x - g^{-1}\nabla C$, and calculate the cost at the new point, $C_{new} = \frac{1}{2}R_{enew}^2$.

2.3.1.4. Parameter determination. If $C_{new} < C$, accept the step, $x = x_{new}$, and set $R_e = R_{enew}$ and $\lambda = \lambda \bullet \lambda_{up}$. Otherwise, reject the step, keep the old parameter guess x and the old residuals R_e, and adjust $\lambda = \lambda \bullet \lambda_{up}$.

2.3.1.5. Check for convergence. If the method has converged, return x as the best estimate parameters. If the method has not yet converged, but the step is accepted, estimate the Jacobian J at the new parameter values. Go to step b).

2.3.2. Choice of the damping parameter (λ)

2.3.2.1. Significance. The choice of λ is crucial to the success rate and efficiency of the LM algorithm.

2.3.2.2. Specific effects. Increasing λ will reduce the step size and vice versa. Therefore, if the step is unacceptable, then λ should be increased until a smaller acceptable step is found. If we accept a step, we decrease λ to increase the step size so that it can proceed faster in the correct descent direction, thereby accelerating convergence.

As shown in Fig. 1, the Gompertz growth trajectory of a xenograft-tumor can be divided into three stages: an exponential growth stage (Stage 1), a linear growth stage (Stage 2), and a saturated growth stage (Stage 3). It should be noted that the entire growth process of the xenograft-tumor includes the avascular growth phase and vascular growth phase, each with its own Gompertz growth trajectory. Since the avascular xenograft-tumor can only grow to a few cubic millimeters and is usually completed within a few days after the transplantation, it is difficult to observe and measure [7]. When the xenograft-tumor is large enough to be observed and measured, it has generally entered the vascular growth phase. Our study focuses on the Gompertz tracking of the growth trajectories of the human-liver-cancer xenograft-tumors in the vascular growth phase.

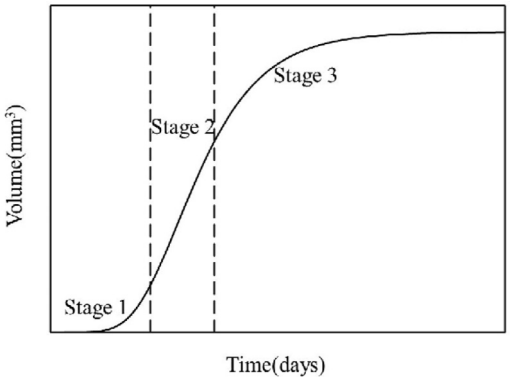

Fig. 1. Three stages of the Gompertz growth trajectory of a xenograft-tumor.

3. Results

The tumor formation rate of the human-liver-cancer xenograft-tumors in the 18 male nude mice was 100%. The measured data

(a) (b)

Fig. 2. Nude mice transplanted with human-liver-cancer xenograft-tumors. (a) A human-liver-cancer xenograft-tumor in the avascular growth phase. (b) A human-liver-cancer xenograft-tumor in the vascular growth phase.

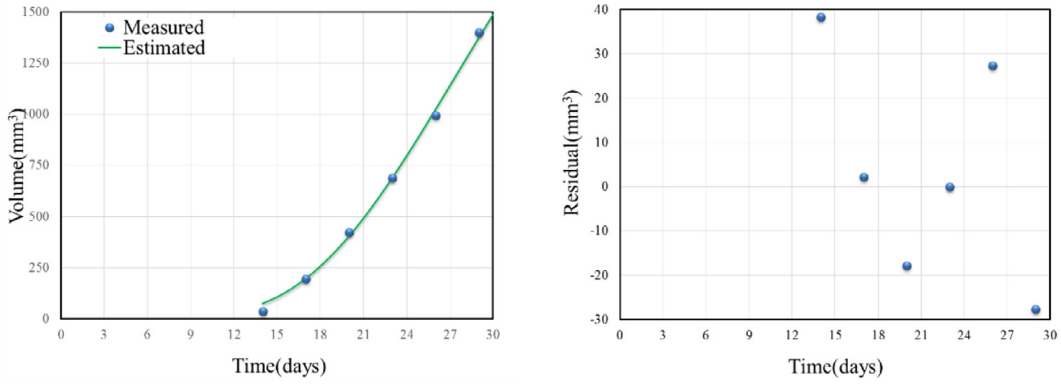

(a) (b)

Fig. 3. Gompertz growth trajectory of the xenograft-tumor in the non-target control group. (a) The measured data points and the Gompertz growth trajectory. (b) The residuals of the Gompertz growth trajectory.

points shown in Figs. 3(a), 4(a) and etc. are from the average data of 6 mice in each group. Fig. 2 shows the nude mice transplanted with human-liver-cancer xenograft-tumors. The avascular xenograft-tumor of human-liver-cancer (not more than a few cubic millimeters) is shown in Fig. 2(a). No obvious changes were observed on the body surface of the nude mouse, and the xenograft-tumor was not touched, let alone measured. The vascularized xenograft-tumor of human-liver-cancer (larger than 10 mm^3) is shown in Fig. 2(b), with a large blue-purple mass on the dorsal side of the nude mouse. The results presented later in this section are all derived from the vascularized xenograft-tumors of human-liver-cancer. According to relevant literature reports, the current studies only used the first 30 days of the volume data of xenograft-tumors, so by convention, we measured and recorded the volume data of xenograft-tumors from day 14 to day 30.

Fig. 3 shows the Gompertz growth trajectory of the xenograft-tumor in the non-target control group. In Fig. 3(a), the blue dots are the six measured data points between day14 and day 30 after transplantation, and the green solid line is the Gompertz growth trajectory. The xenograft-tumor volume measured on day 14 after transplantation was 37.12 mm^3, and it is apparent that the xenograft-tumor is already vascularized. Day 0 to day 13 after transplantation is the transition period of the xenograft-tumor from the avascular growth phase to the vascular growth phase. Fig. 3(b) shows the residuals of the growth trajectory. It should be noted that the partial components of residuals are the errors caused by the measurement and approximate estimation of the xenograft-tumor volume and should not be entirely attributed to the Gompertz model. Based on the model parameters of the Gompertz growth trajectory in Fig. 3(a), we calculated the corresponding growth assessment indicators for the non-target control group: $r = 0.099$ (inhibitory factor); $K = 3204.704$ (carrying capacity); $r\ln K = 0.799$ (promoting factor).

Fig. 4 shows the Gompertz growth trajectory of the xenograft-tumor in the Gsk3β knockdown group. On day 14 after transplantation, the measured xenograft-tumor volume was 3.28 mm^3, which was in the angiogenic phase. On day 17, the measured xenograft-tumor volume was 21.56 mm^3, and it was found that the xenograft-tumor had entered the vascular growth phase. The residual values in Fig. 4(b) are much smaller than those of the non-target control group in Fig. 3(b). Based on the model parameters of the Gompertz growth trajectory in Fig. 4(a), we calculated the corresponding growth assessment indicators for the xenograft-tumor in the Gsk3β knockdown group: $r = 0.057$ (inhibitory factor); $K = 9472.836$ (carrying capacity); $r\ln K = 0.5219$ (promoting factor).

Fig. 5 shows the Gompertz growth trajectory of the xenograft-tumor in the c-Myc knockdown group. The growth of the xenograft-tumor was barely observed during the first 26 days after transplantation, which was in the avascular growth phase or the angiogenic phase. The volume of the xenograft-tumor measured on day 29 was 80.14 mm^3, apparently in the vascular growth phase. The maximum residual in Fig. 5(b) is only −0.18, which is much smaller than those in Figs. 3(b) and 4(b). Based on the model parameters of the Gompertz growth trajectory in Fig. 5(a), we calculated the corresponding growth assessment indicators for the xenograft-tumor in the c-Myc knockdown group: $r = 0.272$ (inhibitory factor); $K = 16{,}000.002$ (carrying capacity); $r\ln K = 2.663$ (promoting factor).

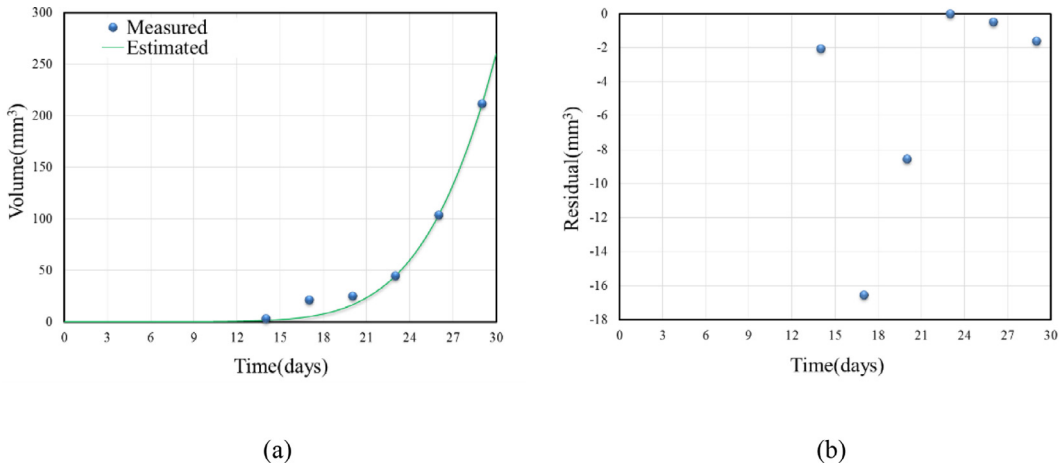

Fig. 4. Gompertz growth trajectory of the xenograft-tumors in the Gsk3β knockdown group. (a) The measured data points and the Gompertz growth trajectory. (b) The residuals of the Gompertz growth trajectory.

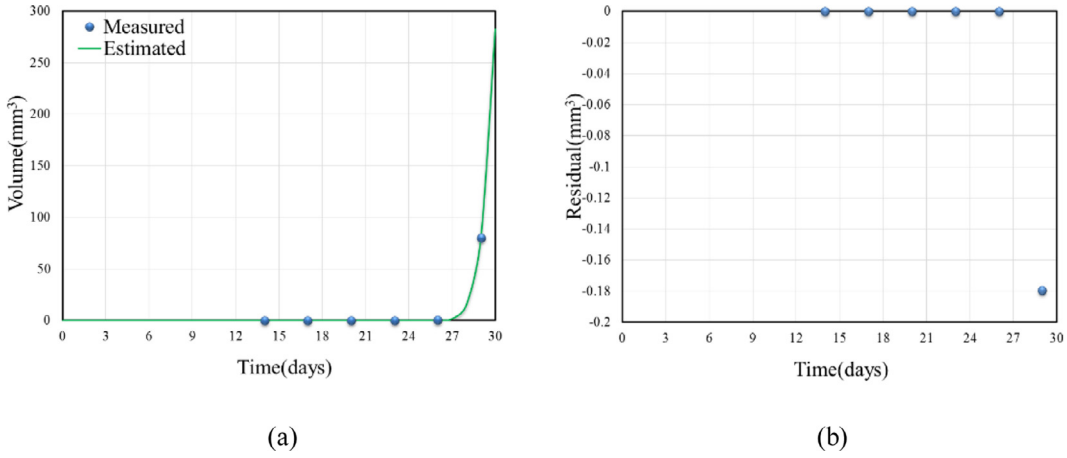

Fig. 5. Gompertz growth trajectory of the xenograft-tumor in the c-Myc knockdown group. (a) The measured data points and the Gompertz growth trajectory. (b) The residuals of the Gompertz growth trajectory.

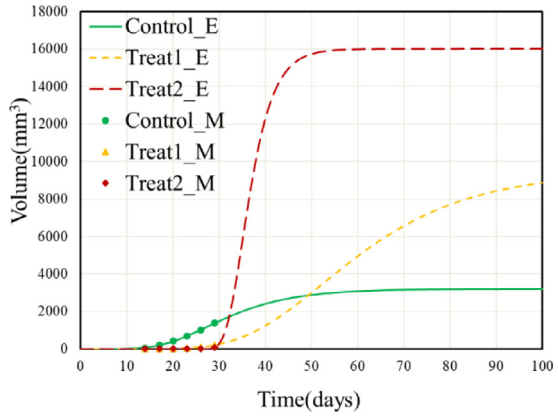

Fig. 6. 100-day Gompertz growth trajectories and the first 30 days of measured volume data of the human-liver-cancer xenograft-tumors in the non-target control, Gsk3β knockdown, and c-Myc knockdown groups.

Fig. 6 shows the 100-day Gompertz growth trajectories (Control_E, Treat1_E, and Treat2_E) of xenograft-tumors, while the first 30 days of measured volume data (Control_M, Treat1_M, and Treat2_M) are plotted as scatter plots. The 100-day Gompertz growth trajectory covers all three growth stages (Stage 1, Stage 2, and Stage 3) of the xenograft-tumor as shown in Fig. 1. It is not difficult to see from Fig. 6 that the growth of the xenograft-tumor in the non-target control group has entered the linear growth stage (Stage 2) on day 30 after transplantation, while the growth of the xenograft-tumors in the Gsk3β knockdown and c-Myc knockdown groups are still in the exponential growth stage (Stage 1). If the data for the saturated growth stage (Stage 3) is required, the xenograft-tumors should grow for a few more days.

4. Discussion

The high mortality rate of liver cancer has become one of the major public health problems threatening human survival [36]. Liver cancer is the second most common cancer after lung cancer in China [37]. The nude mouse model of human-liver-cancer xenograft-tumors is one of the most prevalent and widely used preclinical trial animal models. It is considered the "living test tube" that best reflects the biological characteristics of human liver cancer. It has become an ideal tool for studying the pathophysiology of liver cancer, verifying various methods for the diagnosis and treatment of liver cancer, and screening new anti-liver-cancer drugs [22]. It is an important prerequisite for the effective use of relevant trial results that accurately tracking the growth trajectories of human-liver-cancer xenograft-tumors in nude mice under the intervention of knocking down Gsk3β or c-Myc. At the same time, it also lays a solid mathematical modeling foundation for un-

derstanding the inhibition of liver cancer by knocking down Gsk3β or c-Myc.

It can be seen from Fig. 2 that the size and shape of the xenograft-tumor are very different in the avascular and vascular growth phases. Since this study focuses on the xenograft-tumors in the vascular growth phase, its volumes can be conveniently measured using a vernier caliper. However, due to the limited accuracy of the vernier caliper, it is impossible to measure the volumes of the xenograft-tumor in the avascular growth phase [7]. If there is no measured volume data, there is no basis for the Gompertz tracking of the growth trajectories of avascular xenograft-tumors. Therefore, there is much room for improvement in the method and technique for measuring the volume of avascular xenograft-tumors in the future.

The Gompertz model accurately tracked the growth trajectory of the vascularized xenograft-tumor from day 14 to day 30, as shown in Fig. 3. Compared with the growth curve obtained by directly connecting the measured data points with straight lines in references [26,38], the growth trajectory in Fig. 3 can more accurately estimate or predict the volume size at any time other than the measured data points and also calculate the growth assessment indicators. It is worth mentioning that there are two key prerequisites for obtaining such a high-quality growth trajectory: first, the volumetric measurement errors of the xenograft-tumor must be small enough; secondly, the Gompertz model parameter estimation method is correctly selected. The Lemberg-Marquardt algorithm fully demonstrates its advantages, namely fast convergence and small residual errors. Based on the growth trajectory and carrying capacity, we judge that the effect of the promoting factor on the growth of the xenograft-tumor is greater than that of the inhibitory factor in the non-target control group because the xenograft tumor volume was always increasing rather than decreasing.

Comparing the Gompertz growth trajectories in Figs. 4(a) and 3(a), it is found that knocking down Gsk3β inhibited the growth of the xenograft-tumor. In addition, knocking down Gsk3β also caused the xenograft-tumor in this group to enter the vascular growth phase several days later than that in the non-target control group, which means that knocking down Gsk3β also delayed the angiogenesis of the xenograft-tumor [8,10]. From the growth assessment indicators of the xenograft-tumor, the promoting and inhibitory factors of the Gsk3β knockdown group are smaller than those of the non-target control group, but the carrying capacity of the Gsk3β knockdown group is greater, which means that the effect of knocking down Gsk3β on the inhibitory factor prevails. If judged by the growth assessment indicators, the growth rate and volume of the xenograft-tumor in the Gsk3β knockdown group should be larger than that of the non-target control group, but the opposite is true; and according to the effect of delayed angiogenesis, the growth rate and volume of the xenograft-tumor in the Gsk3β knockdown group should be smaller than those of the non-target control group, which is exactly the fact. Therefore, we believe that the mechanism of knocking down Gsk3β to inhibit the growth of the xenograft-tumor is to delay angiogenesis.

According to the Gompertz growth trajectories in Figs. 3(a), 4(a) and 5(a), knocking down c-Myc inhibited the growth of the xenograft-tumor more obviously, and the time for the xenograft-tumor to enter the vascular growth phase was also later. We repeatedly checked and compared the assessment indicators of the xenograft-tumor and found that knocking down c-Myc greatly increased the promoting factor, inhibitory factor and carrying capacity of this group. Obviously knocking down c-Myc makes the effect of the promoting factor more prominent. Considering the growth assessment indicators and the delay of angiogenesis in combination, we believe that the mechanism of knocking down c-Myc to inhibit the growth of the xenograft-tumor is also the delay of angiogenesis.

Fig. 6 shows the 100-day Gompertz growth trajectories, of which the predicted growth trajectories after day 30 need further experimental verification in the future. The Gompertz growth trajectory of the non-target control group and the growth assessment indicators can be mutually confirmed. The first 30 days of the Gompertz growth trajectories of the Gsk3β knockdown and c-Myc knockdown groups were contrary to the growth assessment indicators but in good agreement with the delay of angiogenesis. The next 70 days of the Gompertz growth trajectories of the Gsk3β knockdown and c-Myc knockdown groups were consistent with the growth assessment indicators and the delay of angiogenesis.

5. Conclusions

In this study, the 18 male specific-pathogen-free (SPF) BALB/c nude mice were randomly divided into three groups and different interventions were performed to establish the non-target control, Gsk3β knockdown, and c-Myc knockdown groups, and the volumes of the xenograft-tumors were measured from day 14 to day 30 after transplantation. The first 30-days and the whole 100-days of Gompertz growth trajectories of the xenograft-tumors were obtained respectively, and the growth assessment indicators of each group were calculated based on the parameters of the Gompertz model.

Our results show that: 1) the Gompertz model can accurately track the growth trajectories of the xenograft-tumors in the non-target control, Gsk3β knockdown, and c-Myc knockdown groups; 2) knocking down Gsk3β or c-Myc can inhibit the growth of xenograft-tumors. It is the combined effect of growth-promoting factor, growth inhibitory factor, and delay of angiogenesis, of which the delay of angiogenesis plays a decisive role; 3) the 100-day Gompertz growth trajectory can provide complete information about the two phases and three stages of xenograft-tumor growth. Therefore, it is strongly recommended that nude mouse trials be extended from 30 days (currently widely accepted) to 100 days.

In conclusion, the Gompertz model can well reveal the growth pattern of the human-liver-cancer xenograft-tumors in nude mice. Combined with the growth assessment indicators obtained from the Gompertz model parameters, one can further clarify the mechanism that affects the growth of xenograft-tumors. The Gompertz tracking of the growth trajectories of the human-liver-cancer xenograft-tumors in nude mice has broad application prospects in the fields of basic research, drug verification, and clinical treatment, etc.

Declaration of Competing Interest

We declare that there is no conflict of interest with any agency or individual.

Acknowledgments

This work was supported by the University of Science and Technology of China [grant numbers YZ2091600009].

References

[1] B. Gompertz, On the nature of the function expressive of the law of human mortality, and on a new method of determining the value of life contingencies, Philos. Trans. R. Soc. Lond. 115 (2) (1825) 513–583.
[2] A.K. LAIRD, Dynamics of tumor growth, Br. J. Cancer 18 (3) (1964) 490–502.
[3] M.A.J. Chaplain, A. Growth, Angiogenesis and vascular growth in solid tumours: the mathematical modelling of the stages of tumour development, Math. Comput. Model. 23 (6) (1996) 47–87.

[4] L. Ferrante, S. Bompadre, L. Possati, L. Leone, Parameter estimation in a gompertzian stochastic model for tumor growth, Biometrics 56 (4) (2000) 1076–1081.
[5] M. Marusic, Z. Bajzer, J.P. Freyer, S. Vukpavlovic, Analysis of growth of multicellular tumour spheroids by mathematical models, Cell Prolif. 27 (2) (1994) 73–94.
[6] Z. Bajzer, M. Marusic, S. VukPavlovic, Conceptual frameworks for mathematical modeling of tumor growth dynamics, Math. Comput. Model. 23 (6) (1996) 31–46.
[7] M.E. Orme, M.A.J. Chaplain, A mathematical model of vascular tumour growth and invasion, Math. Comput. Model. 23 (10) (1996) 43–60.
[8] P. Hahnfeldt, D. Panigrahy, J. Folkman, L. Hlatky, Tumor development under angiogenic signaling: a dynamical theory of tumor growth, treatment response, and postvascular dormancy, Cancer Res. 59 (19) (1999) 4770–4775.
[9] L.E.B. Cabrales, J.I. Montijano, M. Schonbek, A.R.S. Castaneda, A viscous modified Gompertz model for the analysis of the kinetics of tumors under electrochemical therapy, Math. Comput. Simul. 151 (2018) 96–110.
[10] N. Hartung, S. Mollard, D. Barbolosi, A. Benabdallah, G. Chapuisat, G. Henry G, et al., Mathematical modeling of tumor growth and metastatic spreading: validation in tumor-bearing mice, Cancer Res. 74 (22) (2014) 6397–6407.
[11] S. Benzekry, C. Lamont, A. Beheshti, A. Tracz, J.M.L. Ebos, L. Hlatky, et al., Classical mathematical models for description and prediction of experimental tumor growth, PLoS Comput. Biol. 10 (8) (2014) e1003800.
[12] S. Patmanidis, A.C. Charalampidis, I. Kordonis, K. Strati, G.D. Mitsis, G.P. Papavassilopoulos, Individualized growth prediction of mice skin tumors with maximum likelihood estimators, Comput. Meth. Prog. Bio. 185 (2020) 105165.
[13] G. Albano, V. Giorno, P. Roman-Roman, S. Roman-Roman, F. Torres-Ruiz, Estimating and determining the effect of a therapy on tumor dynamics by means of a modified Gompertz diffusion process, J. Theor. Biol. 364 (2015) 206–219.
[14] L.E.B. Cabrales, J.J.G. Nava, A.R. Aguilera, J.A.G. Joa, H.M.C. Ciria, M.M. Gonzalez, et al., Modified Gompertz equation for electrotherapy murine tumor growth kinetics: predictions and new hypotheses, BMC Cancer 10 (2010) 589.
[15] M. Bodnar, M.J. Piotrowska, U. Forys, Gompertz model with delays and treatment: mathematical analysis, Math. Biosci. Eng. 10 (3) (2013) 551–563.
[16] M. Savarin, A. Prevc, M. Rzek, M. Bosnjak, I. Vojvodic, M. Cemazar, et al., Intravital monitoring of vasculature after targeted gene therapy alone or combined with tumor irradiation, Technol. Cancer Res. Treat. 17 (2018) UNSP 1533033818784208.
[17] T.L. Li, G.B. Kang, T.Y. Wang, H. Huang, Tumor angiogenesis and anti-angiogenic gene therapy for cancer (Review), Oncol. Lett. 16 (1) (2018) 687–702.
[18] J.H. Cho, Y.M. Lee, M.F. Starost, B.C. Mansfield, J.Y. Chou, Gene therapy prevents hepatic tumor initiation in murine glycogen storage disease type ia at the tumor-developing stage, J. Inherit. Metab. Dis. 42 (3) (2019) 459–469.
[19] D. Trnski, M. Sabol, A. Gojevic, M. Martinic, P. Ozretic, V. Musani, et al., GSK3β and gli3 play a role in activation of hedgehog-gli pathway in human colon cancer — targeting GSK3β downregulates the signaling pathway and reduces cell proliferation, Biochim. Biophys. Acta-Mol. Basis Dis. 1852 (12) (2015) 2574–2584.
[20] S.G. Gao, S.G. Li, X.X. Duan, Z. Gu, Z.K. Ma, X. Yuan, et al., Inhibition of glycogen synthase kinase 3 beta (GSK3β) suppresses the progression of esophageal squamous cell carcinoma by modifying STAT3 activity, Mol. Carcinog. 56 (10) (2017) 2301–2316.
[21] P.Y. Yang, Y. Jiang, Y. Pan, X.P. Ding, P. Rhea, J.B. Ding, et al., Mistletoe extract fraxini inhibits the proliferation of liver cancer by down-regulating c-Myc expression, Sci. Rep. 9 (2019) 6428.
[22] I. Szadvari, O. Krizanova, P. Babula, Athymic nude mice as an experimental model for cancer treatment, Physiol. Res. 65 (S4) (2016) S441–S453.
[23] H.W.L. Hann, M.W. Stahlhut, R. Rubin, W.C. Maddrey, Antitumor effect of deferoxamine on human hepatocellular carcinoma growing in athymic nude mice, Cancer 70 (8) (1992) 2051–2056.
[24] Y.S. Gao, X.P. Chen, K.Y. Li, Z.D. Wu, Nude mice model of human hepatocellular carcinoma via orthotopic implantation of histologically intact tissue, World J. Gastroenterol. 10 (21) (2004) 3107–3111.
[25] H.M. Li, D.Z. Jiang, L. Zhang, J.Z. Wu, Inhibition of tumor growth of human hepatocellular carcinoma hepg2 cells in a nude mouse xenograft model by the total flavonoids from arachniodes exilis huimin, Evid-Based Complement Altern. Med. (2017) 5310563.
[26] Q.Y. Li, H.Y. Li, C.J. He, Z.H. Jing, C.A. Liu, J. Xie, W.W. Ma, H.S. Deng, The use of 5-fluorouracil-loaded nanobubbles combined with low-frequency ultrasound to treat hepatocellular carcinoma in nude mice, Eur. J. Med. Res. 22 (2017) 48.
[27] K.Q. Han, G. Huang, W. Gu, Y.H. Su, X.Q. Huang, C.Q. Ling, Anti-tumor activities and apoptosis-regulated mechanisms of bufalin on the orthotopic transplantation tumor model of human hepatocellular carcinoma in nude mice, World J. Gastroenterol. 13 (24) (2007) 3374–3379.
[28] B.L. Li, Y.Q. Zhang, W.Z. Wu, G.H. Du, L. Cai, H.C. Shi, S.L. Chen, Neovascularization of hepatocellular carcinoma in a nude mouse orthotopic liver cancer model: a morphological study using X-ray in-line phase-contrast imaging, BMC Cancer 17 (2017) 73.
[29] K. Rygaard, M. Spang-Thomsen, Quantitation and gompertzian analysis of tumor growth, Breast Cancer Res. Tr. 46 (2–3) (1997) 303–312.
[30] S.J. Olshansky, B.A. Carnes, Ever since gompertz, Demography 34 (1) (1997) 1–15.
[31] S. Patmanidis, A.C. Charalampidis, I. Kordonis, G.D. Mitsis, G.P. Papavassilopoulos, Comparing methods for parameter estimation of the gompertz tumor growth model, IFAC Proc. 50 (1) (2017) 12203–12209 20th World Congress of the International-Federation-of-Automatic-Control (IFAC), doi:10.1016/j.ifacol.2017.08.2289.
[32] K. Vuori, I. Stranden, M.L. Sevon-Aimonen, E.A. Mantysaari, Estimation of nonlinear growth models by linearization: a simulation study using a Gompertz function, Genet. Sel. Evol. 38 (4) (2006) 343–358.
[33] K. Amini, F. Rostami, A modified two steps levenberg-marquardt method for nonlinear equations, J. Comput. Appl. Math. 288 (2015) 341–350.
[34] K. Amini, F. Rostami, G. Caristi, An efficient levenberg-marquardt method with a new lm parameter for systems of nonlinear equations, Optimization 67 (2018) 637–650.
[35] A.A. Coelho, Optimum levenberg-marquardt constant determination for nonlinear least-squares, J. Appl. Crystallogr. 51 (2018) 428–435.
[36] F. Bray, J. Ferlay, I. Soerjomataram, R.L. Siegel, L.A. Torre, A. Jemal, Global cancer statistics 2018: globocan estimates of incidence and mortality worldwide for 36 cancers in 185 countries, CA-Cancer J. Clin. 68 (2018) 394–424.
[37] R.X. Zhu, W.K. Seto, C.L. Lai, M.F. Yuen, Epidemiology of hepatocellular carcinoma in the asia-pacific region, Gut. Liver 10 (2016) 332–339.
[38] Y.Y. Chen, C. Chen, Z.M. Zhang, H. Xiao, B.J. Mao, H. Huang, et al., Expression of B-cell translocation gene 2 is associated with favorable prognosis in hepatocellular carcinoma patients and sensitizes irradiation-induced hepatocellular carcinoma cell apoptosis in vitro and in nude mice, Oncol. Lett. 13 (4) (2017) 2366–2372.